Available online at www.sciencedirect.com
SCIENCE DIRECT®
Thermochimica Acta 432 (2005) 254–261
thermochimica acta
www.elsevier.com/locate/tca

Side chain crystallization in microphase-separated poly(styrene-*block*-octadecylmethacrylate) copolymers

E. Hempel[a], H. Budde[b], S. Höring[b], M. Beiner[a,*]

[a] *Department of Physics, Martin-Luther-University Halle-Wittenberg, Hoher Weg 8, D-06099 Halle, Germany*
[b] *Department of Chemistry, Martin-Luther-University Halle-Wittenberg, Hoher Weg 8, D-06099 Halle, Germany*

Received 14 November 2004; received in revised form 5 January 2005; accepted 19 January 2005
Available online 19 February 2005

Abstract

The crystallization behavior of two microphase-separated poly(styrene-*b*-octadecylmethacrylate) block copolymers with lamellar and cylindrical morphology is studied by DSC. The findings are compared with results for a polyoctadecylmetharcylate (PODMA) homopolymer. The situation in the block copolymers is characterized by the occurrence of a confined side chain crystallization in small PODMA domains surrounded by a glassy polystyrene phase. The strength of confinement effects depends significantly on the block copolymer morphology. The crystallization behavior of PODMA lamellae with a thickness of about 10 nm is only slightly affected and similar to the situation in the homopolymer. In cylindrical PODMA domains with a diameter of about 10 nm strong confinement effects are observed: the degree of crystallinity is 50% reduced and the crystallization kinetics slows down. The Avrami coefficients change from $n \approx 3$ for the homopolymer and PODMA lamellae to $n \approx 1$ for PODMA cylinders. This observation indicates one-dimensional growth in small cylinders or a change from heterogeneous to homogeneous nucleation. Pros and cons of both approaches are discussed. A speculative picture explaining qualitatively the differences in the crystallization behavior of PODMA lamellae and cylinders in a glassy polystyrene matrix is presented.

Keywords: Crystallization; Block copolymer; Side chain polymer; Self-assembled confinement; Calorimetry

1. Introduction

An important method to learn more about general aspects of the crystallization process is to study crystallizable liquids and polymers under confinement [1,2]. The most traditional way is to study small droplets of size 50–1000 nm in order to detect changes in the crystallization behavior. This droplet method has been applied already in the 1960s to emulsions of alkanes in water [3] and until now is a powerful tool to investigate the transition from heterogeneous to homogeneous nucleation [4–6]. Crystallizable materials have been also transferred into porous glasses or zeolites with typical pore sizes of 2–50 nm in order to study the influence of smaller confinements [7–10]. More recently the crystallization in microphase-separated block copolymers containing self-assembled domains with a typical dimension of 10–50 nm [1] and in thin polymer films with a thickness of 10–1000 nm [11–14] has been studied in detail. In all cases significant changes in crystallization kinetics and morphology have been observed. Although thin polymer films arranged on top of a substrate and thin self-assembled lamellae in block copolymers differ in many details the crystallization behavior is affected in a similar way. Both methods are alternative approaches to follow the crystallization under confinement. This shows that the crystallization process in microphase-separated block copolymers has a lot of similarities to the crystallization in thin polymer films which is studied by modern calorimetric techniques recently [14,15] and in other papers of this special issue [16].

Polymer crystallization in small domains of microphase-separated block copolymers has been extensively studied by scattering techniques, calorimetry and relaxation spectroscopy [1]. The influences of different self-assembled

* Corresponding author. Tel.: +49 345 552 5350; fax: +49 345 552 7351.
E-mail address: beiner@physik.uni-halle.de (M. Beiner).

0040-6031/$ – see front matter © 2005 Elsevier B.V. All rights reserved.
doi:10.1016/j.tca.2005.01.037

constraints on crystallization kinetics and nucleation process have been investigated [17–20]. The inter-relation between crystallization process and microphase separation is a closely related question. Most of the previously studied diblock copolymers consist of one crystallizable and one amorphous component. Considering the relation between the glass temperature T_g of the amorphous block and the crystallization temperature of the other component different situations have been studied: T_g can be significantly higher than the crystallization temperature T_c of the other component so that small domains of size 10–50 nm crystallize in a rigid environment. In other cases T_g is comparable to T_c so that the crystallization process can influence the microphase morphology of the relatively soft and mobile block copolymer. Basically block copolymers where main chains of one component are able to crystallize have been studied so far. In these polymers chain folding occurs during the crystallization process. Well investigated is the crystallization of polyethyleneoxide, polyethylene and poly(ϵ-caprolactone) in block copolymers like poly(ethyleneoxide-*b*-butadiene) [19,20], poly(ethyleneoxide-*b*-propyleneoxide) [21], poly(ethyleneoxide-*b*-styrene) [22], poly(ethyleneoxide-*b*-butyleneoxide) [23], poly(ethylene-*b*-propylene) [24], poly(ethylene-*b*-vinylcyclo-hexane) [17,25], poly-(ethylene-*b*-styrene) [26], poly(ethylene-*b*-ethylethylene) [25,27], and poly(ϵ-caprolactone-*b*-butadiene) [28].

The crystallization of *side chain polymers* under confinement has not been investigated in detail so far. A special feature of the crystallization of alkyl groups in side chain polymers is that crystallization starts from a nanophase-separated melt [29], i.e. long alkyl groups are already aggregated before crystallization starts to occur. Alkyl nanodomains with a typical dimension of 1–3 nm depending on the length of the alkyl groups, are formed. These alkyl nanodomains undergo during the crystallization process a transition from the disordered to the partly crystalline state [30]. The consequence for microphase-separated block copolymers containing such side chain polymers as one component is the existence of a hierarchy of two length scales: one is due to nanophase separation of the side chain polymer on a scale in the 1 nm range and the other one is due to microphase separation of both block copolymer components on scales of about 10 nm. Recently, results are reported for block copolymers with one component being a liquid-crystalline side chain polymer showing similar features [31–34].

In this paper we present calorimetric results for microphase-separated poly(styrene-*b*-octadecyl methacrylate) copolymers, P(S–*b*–ODMA), with different composition and morphology. The crystallizable component here is a side chain polymer, PODMA, where long alkyl groups with 18 carbon atoms in each monomeric unit crystallize in small alkyl nanodomains with a typical dimension of about 2 nm. The situation in the investigated P(S–*b*–ODMA) copolymers is characterized by $T_g \gg T_m \approx T_c$ (Fig. 1), i.e., crystallization of the PODMA block occurs always in a rigid environment formed by the glassy polystyrene phase. It will be interesting to see whether or not basic features of the side chain crystallization in our block copolymers are similar to recent findings for long main chains which crystallize in self-assembled block copolymer domains.

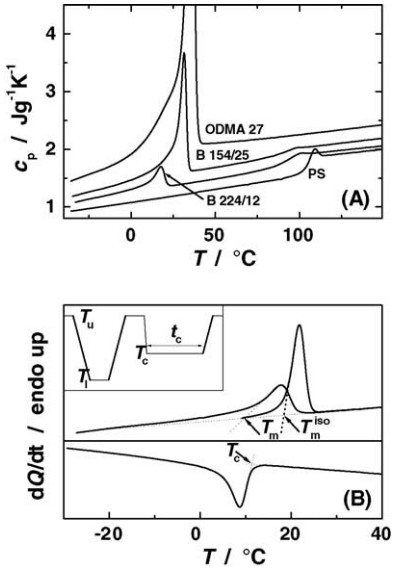

Fig. 1. (A) Temperature-dependent heat capacity for two P(S-*b*-ODMA) block copolymers as well as PS and PODMA homopolymers. Heating rate is +20 K/min after a cooling run with the same rate. (B) Heat flow rate for the B224/12 sample measured during cooling and heating with 10 K/min. The determined onset temperatures are indicated. The insert shows the temperature-time program of the DSC measurements. T_u is chosen to be ≈20 K above T_m of the PODMA block and ≈40 K lower than T_g of the PS block. T_l is always −30 °C. The samples are cooled with a rate of −40 K/min to the isothermal crystallization temperature T_c. T_c and the isothermal crystallization time t_c are varied in a wide range to obtain information about the crystallization kinetics. The heat of melting $q_m(T_c, t_c)$ is determined from the peak area between measured dQ/dt curve and the base line extrapolated from the liquid state.

2. Experimental

2.1. Sample synthesis

The investigated poly(S–*b*–ODMA) copolymers are synthesized by anionic polymerization. Styrene (Merck) was destabilized, dried over CaH_2 and distilled from dibutyl magnesium. Octadecylmethacrylate (Merck) was dissolved in dry THF (Merck) and stirred over CaH_2 for a few days. The solution was subsequently filtrated over silica gel to remove stabilizer and the solvent was evaporated in vacuum. THF was dried over CaH_2 and freshly distilled from the purple sodium salt of the benzophenone dianion. All other solvents were dried and distilled by standard procedures. 1,1-Diphenylethylene (Merck) was dried with a few drops of *sec*-butyl lithium and distilled. The experiments were performed under argon, purified by Oxisorb and Hydrosorb (Messer-Grießheim). Initiator *S*-butyl lithium (Aldrich) and other reagents were used as received.

Table 1
Sample characterization

Sample	Type	Φ_{ODMA}	$\bar{M}_n$(kg/mol)	$\bar{M}_w/\bar{M}_n$	d_{ODMA}(nm)	Δc_p (J/gK)	T_g (°C)
ODMA27	Homopolymer	1	9.0	2.1	-	–	–
B154/25	Lamellar	0.39	24.4	1.1	8.7	0.13	84
B224/12	Cylindrical	0.18	27.6	1.1	10.9	0.22	84

All polymerizations were carried out in carefully flamed glass reactors in THF as the solvent at −78 °C (styrene polymerization) or 0 °C (octadecylmethacrylate polymerization) under an argon atmosphere using syringe techniques. After several cycles of degassing the solvent was transferred to the reactor by condensation from oligomeric polystyrene anions under reduced pressure. Then the desired amount of monomer was added followed by the initiator. After 1 h the living polystyrene anions were end-capped with diphenylethylene and stirred for another 15 min. Octadecylmethacrylate as the second monomer was added drop-wise. Then the solution was warmed to 0 °C and stirred for several hours. The reaction was terminated by adding methanol. The polymer was precipitated in ethanol at room temperature, washed and dried in vacuum for several days.

The PODMA homopolymers are synthesized by anionic polymerization. The PS sample is a commercial product by BASF (PS 168N). The octadecane sample is a commercial product by Aldrich.

2.2. Sample characterization

The parameters characterizing the microstructure of our polymers are summarized in Table 1. Molecular weight parameters are determined by size exclusion chromatography (SEC) using a Knauer instrument with a RI-detector and a standard column (Macherey & Nagel) calibrated with PS-standards. The composition of the diblock copolymers was determined based on ^{1}H-NMR measurements using a Varian spectrometer (400 MHz) in chloroform-d. The volume fractions are calculated using the densities for PS ($\rho_{PS} = 1.04\,g/cm^3$, cf. Ref.[35]) and PODMA ($\rho_{PODMA} = 0.865\,g/cm^3$, cf. Ref. [36]) homopolymers.

The two copolymers studied in this paper by DSC show lamellar (B154/25) and cylindrical (B224/12) morphology, respectively. Microphase-separated samples are prepared from the melt by annealing at 150 °C under vacuum for 24 h. The homopolymers are prepared analogously. Morphology and size of the PODMA domains (Table 1) are determined based on X-ray scattering measurements performed on beamline BM24 at the European Synchrotron Radiation Facility in Grenoble and experiments on a home-made setup based on a HI-Star detector combined with a RIGAKU rotating anode emitting Cu Kα radiation ($\lambda = 0.1542$ nm). Further details of the setup used and the scattering experiments are described elsewhere [37,38].

A Pyris Diamond DSC and a DSC 7 from Perkin-Elmer are used for the calorimetric experiments. The applied time-temperature program is shown in the insert of Fig. 1B. Typical cooling and heating curves as well as methods to determine crystallization temperature (T_c), melting temperature (T_m) and to estimate the heat of melting (q_m) are shown in Fig. 1B. An onset construction is used for the determination of T_c and T_m in order to minimize the influence of experimental effects like temperature gradients in the sample. The reported trends are basically independent on this choice. T_c and T_m values obtained from the peak maxima indicate similar behavior.

3. Results

A comparison of conventional $c_p(T)$ curves as obtained from heating scans on the two microphase-separated P(S–*b*–ODMA) copolymers with cylindrical (B224/12) and lamellar morphology (B154/25) with that for the corresponding homopolymers, poly(*n*-octadecylmethacrylate) and polystyrene, shows that melting of the PODMA block as well as glass transition of the PS block occur in a similar temperature range as in the homopolymers (Fig. 1A). The Δc_p values for the PS glass transition correspond approximately to the PS content as expected for block copolymers in the microphase-separated state (Table 1). An analysis of the melting peaks in heating curves ($dT/dt = +10$ K/min) shows that crystallization temperature T_c and degree of crystallinity D_c of PODMA lamellae with a thickness of about 10 nm and PODMA homopolymer are very similar. The D_c values are estimated here based on the equation $D_c = q_m/q_{m,CH_2}$ with $q_{m,CH_2} = 3.4$ kJ/mol being the heat of melting per CH_2 unit as obtained from DSC measurements on octadecane. This q_{m,CH_2} value is very similar to the average value reported for alkanes elsewhere [39]. This method to determine D_c based on the assumption that the heat of melting per CH_2 unit is identical to that of alkanes. The situation in PODMA cylinders with a diameter of about 10 nm is characterized by reduced T_c and T_m values as well as significantly ($\approx$ 50%) smaller degrees of crystallinity D_c of the PODMA block (Table 2). This is a first indication that there are strong confinement effects in cylindrical PODMA domains while such effects are less pronounced for the lamellar P(S–*b*–ODMA) block copolymer.

A comparison of the crystallization and melting temperatures, T_c and T_m, shows that the differences between both temperatures are relatively small, $T_m - T_c = 1 \ldots 7$ K. The ratio $u = (T_m - T_c)/T_m$ often used to quantify undercooling is $0.005 < u < 0.022$ (Table 2). Note, that this value is not strongly affected by the morphology of the investigated block copolymer and that the reported values are similar to the values reported for alkanes with comparable length

Table 2
Calorimetric parameters of the crystallization process

Sample	q_m (J/g)	D_c	T_m[a]	T_c[a]	$\Delta T/T_m$[b]	n[c]	$\Delta \log t_c$ (decades)	$d \log \tau_c/dT_c$ (decades/K)	$dD_c/d \log t_c$ (mol%/decade)
ODMA27	56	31	32	25	0.018	2.8	0.5	0.43	3.0
B154/25	45	25	28	22	0.022	2.8	0.5	0.64	2.2
B224/12	28	15	11	11	0.005	0.65	2.0	0.77	2.1

[a] Onset temperatures.
[b] Calculated using onset temperatures measured with a rate of $dT/dt = \pm 1$ K/min. All other parameters are taken from heating and cooling curves measured with a rate of $dT/dt = \pm 10$ K/min.
[c] Taken from the inserts of Fig. 5.

$u < 0.004$ [4]. These u values are remarkable smaller than those for other small molecules and conventional polymers where chain folding takes place.

Next step was a study of the isothermal crystallization behavior of the PODMA homopolymer and both block copolymers by DSC. The samples were cooled down rapidly with a rate of $dT/dt = -40$ K/min from the molten state to the crystallization temperature T_c and isothermal scans are performed. These isothermal scans include the information about the crystallization kinetics (Fig. 2). There are obviously significant differences between the behavior of the block copolymer with cylindrical morphology and PODMA homopolymer as well as PODMA lamellae. The later two behave quite similar and show a pronounced peak in isothermal data for the heat flow rate dQ/dt as function of crystallization time t_c. This peak shifts to larger t_c values and broadens with increasing crystallization temperature. Similar behavior is typical for crystal growth in three dimensions [1] but has been reported also for the two-dimensional growth in block copolymer lamellae [25]. The increase is usually attributed to the growth of heterogeneously nucleated crystallites while the decrease at longer times indicates that different crystallites disturb each other and primary crystallization comes to an end. The isothermal heat flow rate for PODMA cylinders in a glassy environment is characterized by a continuous decrease with crystallization time t_c. Similar behavior was reported for the confined crystallization in other block copolymers with isolated domains [22,40] where homogeneous nucleation and/or one-dimensional growth occur.

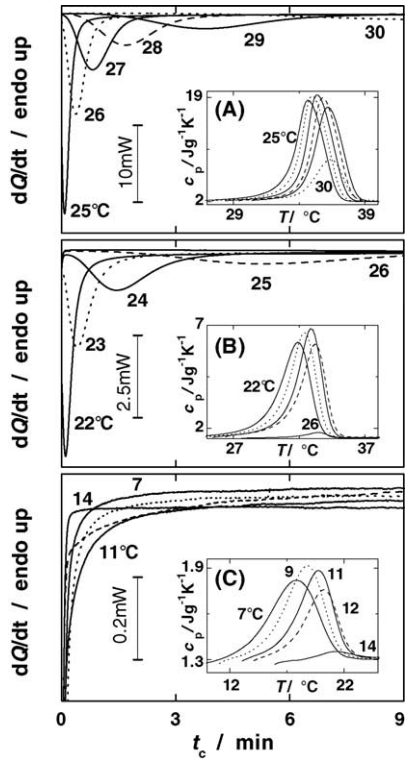

Fig. 2. Heat flow rate dQ/dt measured during isothermal crystallization at the indicated crystallization temperatures T_c for homopolymer (A) as well as block copolymers with lamellar (B) and cylindrical (C) morphology. The inserts show melting curves after isothermal crystallization for $t_c = 10$ min at T_c.

Characteristic crystallization times τ_c can be determined from the heat flow rate data in Fig. 2. For the homopolymer and PODMA lamellae the peak maximum corresponds to τ_c. In case of the B224/12 sample (Fig. 2C) τ_c values can be estimated plotting $\ln(dQ/dt)$ versus t_c assuming that a exponential decay ($dQ/dt \propto \exp(-t_c/\tau_c)$) describes the data [20]. However, this assumption is not really fulfilled for our sample with cylindrical morphology (see below). A stretched exponential decay is observed. This causes uncertainties in the obtained τ_c values. An additional problem is that the baseline reproducibility of the instruments (about 10 μW) is of the same order of magnitude as the tiny contribution coming from the sample in this case. Nevertheless, the obtained τ_c values seem to be in reasonable agreement with τ_c values determined by another method as shown at the end of this section.

An alternative experiment to detect changes during isothermal crystallization at T_c is to perform heating scans after different crystallization times t_c. One gets melting curves as shown in the inserts of Fig. 2. Analyzing the melting peaks in scans after different periods of isothermal crystallization one obtains the heat of melting as function of crystallization time and temperature $q_m(t_c, T_c)$. In Fig. 3 the q_m values are plotted against $\log t_c$ for different temperatures. Heat of melting q_m and degree of crystallinity D_c—estimated from the melting peak area—increase systematically with crystallization time and show a sigmoidal increase plotted versus $\log t_c$. Obviously, primary crystallization occurs in much broader time interval for the B224/12 sample with a cylindrical morphology compared to the B154/25 sample with a lamellar morphology and the PODMA homopolymer. This observa-

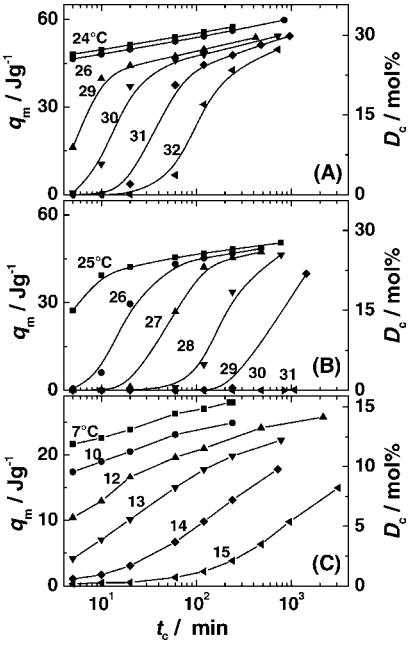

Fig. 3. Heat of melting q_m and degree of crystallinity D_c vs. crystallization time t_c measured at different temperatures T_c for homopolymers (A) as well as block copolymers with lamellar (B) and cylindrical (C) morphology (time-temperature program cf. Fig. 1B).

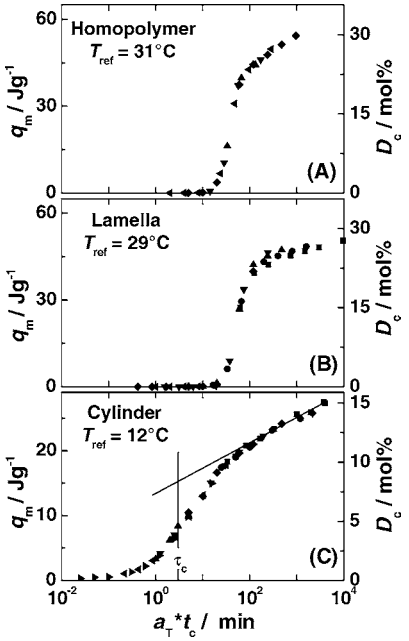

Fig. 4. Master curves for homopolymer (A) and block copolymers with lamellar (B) and cylindrical (C) morphology as constructed from q_m isotherms in Fig. 3. The reference temperatures T_{ref} are indicated. The method to determine the crystallization time τ_c (half-time) from a tangent construction is shown.

tion for the PODMA cylinders is related to a smaller Avrami coefficient as discussed below. Characteristic crystallization times τ_c (half-times) can be obtained in a small temperature interval from the isotherms based on a tangent construction (Fig. 4C). As expected the τ_c values increase rapidly with increasing crystallization temperature T_c.

A method to get characteristic crystallization times τ_c in a wider temperature range based on isothermal q_m data as shown in Fig. 3 is to shift the curves [41] for different crystallization temperatures horizontally in order to get a master curve (Fig. 4). A reference temperature T_{ref} is chosen and all other q_m isotherms are shifted along the $\log t_c$ axis until they superimpose as good as possible. This method is based on the observation that the shape of the $q_m(t_c)$ curves at different temperatures is similar and neglects a small but systematic change in the step height with temperature. The obtained shift factors a_T contain the information about the temperature dependence of τ_c. Knowing the characteristic crystallization time for one reference temperature T_{ref} the τ_c values for all temperatures can be taken out. The results correspond nicely to the τ_c values obtained directly from isothermal dQ/dt scans in Fig. 2. This consistency will be shown below (cf. Fig. 6). Analyzing the shape of the master curves for different samples one observes clear differences. Data for homopolymer and PODMA lamellae indicate that primary crystallization occurs in a narrow time interval of only 0.5 decades, the interval estimated for small PODMA cylinders is about two decades. These values for the width of the transition interval, $\Delta \log t_c$, are obtained from a tangent construction as shown in Fig. 5C. In all samples primary crystallization is followed by a secondary crystallization process. In the course of this secondary process the heat of melting q_m increases on logarithmic time scales linearly. The slope which characterizes the secondary crystallization is system-dependent and varies in the range $dD_c/d \log t_c = 2 \ldots 3$ mol%/decade. The value for the homopolymer is larger than the values for both block copolymers (Table 2). Note, that in all cases the onset temperature of the melting peak T_m increases significantly during the secondary crystallization process. A shift of about $2 \ldots 3$ K/decade is observed.

Isothermal data for the primary crystallization are often analyzed based on the so-called Avrami equation [1]

$$X = 1 - \exp(-kt_c^n) \quad (1)$$

with X being the normalized degree of crystallinity, n the Avrami coefficient, and k being the crystallization rate. In order to determine the Avrami coefficient n one can normalize the $q_m(t_c)$ curves based on a tangent construction as shown in Fig. 4C and fit these data directly to the Avrami equation (Eq. (1)). Normalized degrees of crystallinity $X(\log t_c)$ and the corresponding fits are shown in the inserts of Fig. 5. Alternatively one can plot $\ln(-\ln(1-X))$ versus $\ln t_c$ and determine the slopes corresponding to the Avrami coefficients in these plots (Fig. 5). Consistent Avrami coefficients are obtained by both methods. Clear trends appear (Table 2): (i) Avrami coefficients of the order of $n \approx 3$ are obtained for the homopolymer and the lamellar B154/25 block copolymer. Similar values are obtained usually for crystal growth in two or three dimensions [1,25]. (ii) The Avrami coeffi-

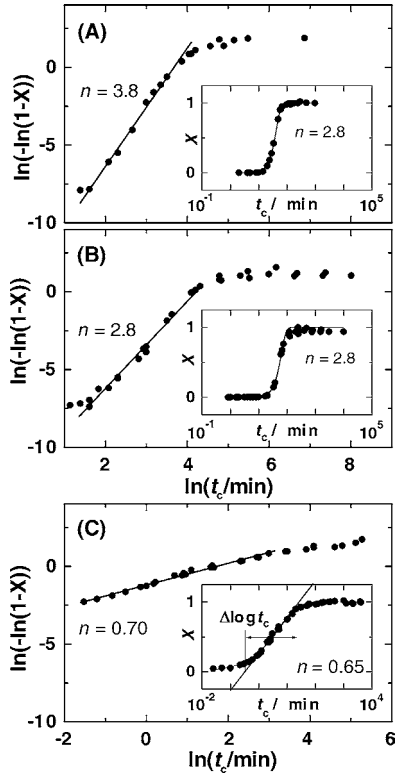

Fig. 5. Avrami plots $\ln(-\ln(1-X))$ vs. $\ln t_c$ for homopolymer (A) as well as block copolymers with lamellar (B) and cylindrical (C) morphology. The normalized degree of crystallinity $X(t_c)$ values are obtained from the master curves in Fig. 4 after correction for the secondary crystallization process by the tangent construction indicated in Fig. 4C. The inserts show normalized degree of crystallinity X vs. crystallization time t_c. The bold lines are fits to the Avrami equation (Eq.(1)). The tangent construction used to determine the width of the transformation range $\Delta \log t_c$ is indicated in the insert of Fig. 5C.

cient for the B224/12 sample with a cylindrical morphology is $n \leq 1$. Such values are an argument for the occurrence of one-dimensional growth often observed in combination with homogeneous nucleation in small isolated domains.

A comparison of the characteristic crystallization times τ_c obtained using two different methods with that for octadecane—the alkane with the same number of carbons as the crystallizable alkyl groups in PODMA—and for other polymers like polyethylene and poly(ϵ-caprolactone) is shown in Fig. 6. The slope for the PODMA homopolymer is $\mathrm{d}\log\tau_c/\mathrm{d}T_c \approx 0.43$ decades/K while $\mathrm{d}\log\tau_c/\mathrm{d}T_c \approx 0.64$ decades/K and $\mathrm{d}\log\tau_c/\mathrm{d}T_c \approx 0.77$ decades/K are obtained for PODMA lamellae and cylinders, respectively. The temperature dependence of τ_c for octadecane is stronger (cf. Fig. 6). The slope for polyethylene ($\mathrm{d}\log\tau_c/\mathrm{d}T_c \approx 0.35$) which crystallizes at significantly higher temperatures is only slightly smaller. This is somehow noticeable because chain folding plays an important role in polyethylene (PE) while it is absent in case of PODMA and octadecane. Data for poly(ϵ-caprolactone) (PCL)—being another polymer with chain folding are included for comparison in Fig. 6 and show that the temperature dependence of τ_c is relatively weak for

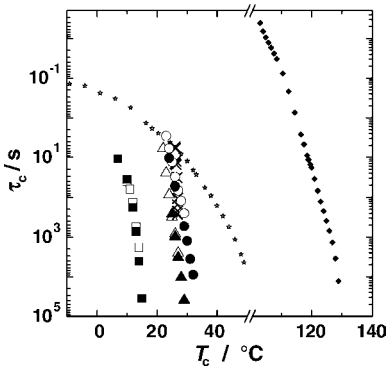

Fig. 6. Crystallization times τ_c for homopolymer (circles) and block copolymer with lamellar (triangles) and cylindrical (squares) morphology as function of crystallization temperature T_c compared with data for octadecane (crosses) and the results for PE (diamonds) and PCL (stars) from Ref.[42]. Full symbols correspond to half-times obtained from $q_m(T_c, t_c)$ (Figs. 3 and 4). Open symbols are τ_c values determined from $\mathrm{d}Q/\mathrm{d}t$ curves measured during isothermal crystallization (Fig. 2).

this sample. Note, that the data for PE and PCL are extended over an extremely wide range of crystallization times. These data are taken from recent measurements by Schick et al. [42] using conventional DSC in combination with modern methods of thin-film calorimetry [16] and indicate the advantages of such methods in this field.

4. Discussion

The presented results show clearly the existence of strong confinement effects in cylindrical PODMA domains with a diameter of about 10 nm while the crystallization behavior of PODMA in lamellae with approximately the same thickness is similar to that of PODMA homopolymers. Main effects of the constraints in case of cylindrical PODMA domains are a significant reduction of the degree of crystallinity D_c and a slowing down of the crystallization kinetics.

A speculative picture explaining these observations for our P(S–*b*–ODMA) block copolymers is presented in Fig. 7. The fact that the side chain crystallization in lamellae is similar as in PODMA hompolymers might be a consequence of the planar PS-PODMA interfaces which do not influence the side chain crystallization significantly. The lamellar morphology seems to match to the shape of the crystallites formed in PODMA and does not disturb the crystallization of alkyl groups. This is consistent with recent X-ray scattering data indicating that the small-scale structure in the PODMA domains is not changed basically compared to the situation in the homopolymer. In case of small PODMA cylinders the PS-PODMA interfaces are strongly curved and reduce obviously the ability of the alkyl groups to crystallize. The shape of the crystallites does not match to the curved interfaces and the immobile glassy polystyrene matrix cannot be deformed easily during the fast crystallization process. Further details of the small scale structure inside the PODMA domains must

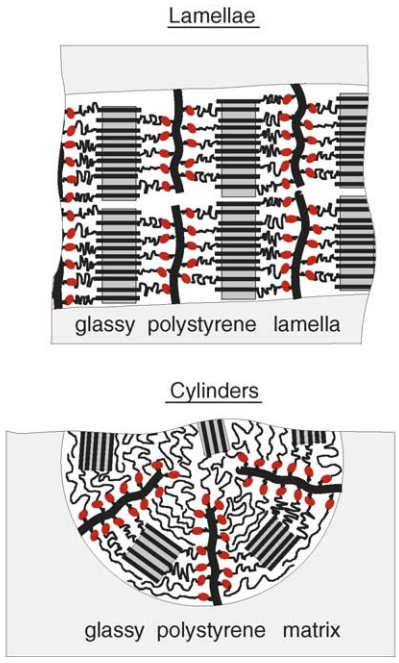

Fig. 7. Schematic picture for the internal structure of PODMA lamellae and cylinders in microphase-separated P(S-*b*-ODMA) copolymers. The dark gray regions indicate crystalline alkyl groups within the PODMA domains. The small beads represent the carboxyl groups of the ODMA units.

be puzzled out based on scattering data showing structural aspects of the crystallization in P(S–*b*–ODMA) block copolymers with different morphology more directly.

Comparing the findings for our crystallizable side chain polymers under confinement with those for other microphase-separated block copolymers where chain folding is important one observes a lot of similarities. Obviously, there are common aspects of the crystallization in small isolated domains embedded in a glassy matrix with a sufficiently higher glass temperature T_g. Main effects are obtained independent on the question whether or not chain folding occurs during the crystallization: (i) in small cylindrical domains the degree of crystallinity is reduced in both cases; (ii) parameters describing the crystallization kinetics like the Avrami coefficient n are similarly affected. Avrami coefficients of $n \approx 3$ are often observed for lamellar block copolymers. Such values are usually interpreted in the sense of a two- or three-dimensional growth of crystallites [25,41]. Avrami coefficients of the order of $n \approx 1$ are typical for cylindrical domains. A decay in dQ/dt data measured during isothermal crystallization supports this observation.

The small Avrami coefficients $n \approx 1$ as obtained in case of PODMA cylinders are consistent with a one-dimensional growth of the crystallite without significant change of the surface area on the growth front. Speculatively, $n \approx 1$ could be also an indication for the occurrence of homogeneous nucleation. Comparable Avrami coefficients are reported, e.g. for a poly(butadiene–*b*–ethyleneoxide) block copolymer with isolated polyethyleneoxide spheres [19,20]. In this case homogeneous nucleation is verified by spatially resolved atomic force microscopy measurements. However, there is one significant difference between calorimetric data for our block copolymer containing PODMA cylinders and block copolymers where homogeneous crystallization of long main chains is observed. Homogeneous crystallization is usually accompanied by large undercooling. $T_m - T_c$ values of about 50 K are typical and a significant increase in $T_m - T_c$ compared to the corresponding homopolymers is observed [20]. This behavior is understood as an intrinsic feature of the homogeneous nucleation within isolated nanodomains. The undercooling in our P(S–*b*–ODMA) copolymers with cylindrical domains having a diameter of only 10 nm, however, is surprisingly not larger but slightly reduced compared to PODMA homopolymer (Table 2). This is unexpected in case of a transition to homogeneous nucleation. In general, the undercooling values for our PODMA containing systems are small, $T_m - T_c < 7$ K or $(T_m - T_c)/T_m < 0.022$ (Table 2). These values are only a bit larger than the values reported for non-folded alkanes with a length of 16 . . . 40 units in the non-emulsified (bulk) state: $T_m - T_c < 1.2$ K or $(T_m - T_c)/T_m < 0.004$ [4]. Small undercooling values are a special feature of the crystallization of alkanes like the occurrence of rotator phases and surface freezing effects [4,43,44]. Based on this observation one could speculate about similarities between the crystallization of alkanes and alkyl groups in side chain polymers [30]. Clear is that alkanes show a significant larger undercooling if homogeneous nucleation occurs in external confinements: experiments in droplets of size of 50–5000 nm [3–5] show $T_m - T_c \approx 12$ K ($(T_m - T_c)/T_m \approx 0.045$) and even larger values are indicated for alkanes in nanoporous glasses with pore diameters in the 10 nm range [10]. In the light of these results it is less plausible to assume that there is a transition from heterogeneous to homogeneous nucleation going from PODMA homopolymers to small isolated PODMA cylinders. The large undercoolings usually observed for the crystallization in isolated domains are missing in case of our B224/12 sample with cylindrical morphology. The huge number of cylinders, however, seems to support homogeneous nucleation.

In the context of the Gibbs–Thomson relation $(T_m^0 - T_m)/T_m^0 \propto 1/L$ with L being the crystal thickness and T_m^0 the melting temperature of a crystal with infinite thickness ($L \to \infty$) the smaller melting temperature T_m for the PODMA cylinders might be related to the smaller degree of crystallinity D_c for this sample. However, making use of this approach would require that the change in the degree of crystallinity is basically due to a change in crystal thickness. This seems to be an oversimplified model. Structural data for the B224/12 sample with cylindrical morphology support the speculative picture shown in Fig. 7 where some of the alkyl groups are unable to crystallize in the conventional way. Moreover, it should be mentioned that the conceptional idea of the Gibbs–Thomson relation is based on equilibrium thermodynamics. Semi-crystalline polymers are kinetically hindered systems in a non-equilibrium state which are able to reorganize [2,45]. Nevertheless, main aspects of crystal-

lizable systems, especially of non-folded *n*-alkanes [39], are described by the Gibbs–Thomson relation often quite well.

Finally, we should note that we cannot really decide based on calorimetric information about the crystallization kinetics in PODMA lamellae and cylinders alone whether confinement influences more crystal growth or nucleation behavior. Most of the arguments are indirect. A final discussion of this issue requires a comparison of results from different methods on a broader class of samples including P(S–*b*–ODMA) block copolymers with a spherical morphology. Work along this line is in progress and will be published in the near future. Calorimetric experiments on thin films, enabling extremely high cooling and heating rates, might be an interesting approach to contribute to this discussion.

5. Conclusions

The presented crystallization experiments on P(S–*b*–ODMA) block copolymers with lamellar and cylindrical morphology by DSC indicate strong confinement effects in PODMA cylinders while the crystallization behavior in lamellae is quite similar to that of PODMA homopolymers. In cylindrical PODMA domains with a diameter of about 10 nm the degree of crystallinity is significantly reduced and the kinetics of the side chain crystallization process is slowed down. This behavior is similar to the findings for crystallizable main chains in small isolated domains embedded in a glassy matrix. The decay in dQ/dt data measured during isothermal crystallization and small Avrami coefficients $n \leq 1$ can indicate either one-dimensional crystal growth in PODMA cylinders or a transition from heterogeneous to homogeneous nucleation. Homogenous nucleation might be expected due to the large number of domains. The small undercooling, however, seems to be an argument against this explanation. More structural information is required to qualify speculative pictures suggested for P(S–*b*–ODMA) block copolymers with lamellar and cylindrical morphology which are consistent with the observations from the DSC experiments reported in this paper.

Acknowledgements

The authors thank Thomas Thurn-Albrecht for helpful discussions. Financial support by the Deutsche Forschungsgemeinschaft (SFB 418) and the ESRF in Grenoble is acknowledged.

References

[1] I.W. Hamley, The Physics of Block Copolymers, Oxford University Press, Oxford, 1998.
[2] J.U. Sommer, G. Reiter, Polymer Crystallization–Observations Concepts and Interpretations, Springer, Berlin, 2002.
[3] D. Turnbull, R.L. Cormia, J. Chem. Phys. 34 (1961) 820.
[4] H. Kraack, E.B. Sirota, M. Deutsch, J. Chem. Phys. 112 (2000) 6873.
[5] R. Montenegro, M. Antonietti, Y. Mastai, K. Landfester, J. Phys. Chem. B 107 (2003) 5088.
[6] M.V. Massa, K. Dalnoki-Veress, Phys. Rev. Lett. 92 (2004) 255509.
[7] C.L. Jackson, G.B. McKenna, Chem. Mater. 8 (1996) 2128.
[8] A. Schreiber, I. Ketelsen, G.H. Findenegg, Phys. Chem. Chem. Phys. 3 (2001) 1185.
[9] C. Alba-Simionesco, G. Dosseh, E. Dumont, B. Frick, B. Geil, D. Morineau, V. Teboul, Y. Xia, Eur. Phys. J. E 12 (2003) 19.
[10] P. Huber, D. Wallacher, J. Albers, K. Knorr, Europhys. Lett. 65 (2004) 351.
[11] M.V. Massa, K. Dalnoki-Veress, J.A. Forrest, Eur. Phys. J. E 11 (2003) 191.
[12] G. Reiter, J.U. Sommer, Phys. Rev. Lett. 80 (1998) 3771.
[13] K. Dalnoki-Veress, J.A. Forrest, M.V. Massa, A. Pratt, A. Williams, J. Polym. Sci.: Polym. Phys. 39 (2001) 2615.
[14] A.T. Kwan, M.Y. Efremov, E.A. Olson, F. Schiettekatte, M. Zhang, P.H. Geil, L.H. Allen, J. Polym. Sci.: Polym. Phys. 39 (2001) 1237.
[15] A.A. Minakov, D.A. Mordvintsev, C. Schick, Polymer 45 (2004) 3755.
[16] Thermochim. Acta, other papers in this issue.
[17] Y.L. Loo, R.A. Register, A.J. Ryan, Phys. Rev. Lett. 84 (2000) 4120.
[18] Y.L. Loo, R.A. Register, A.J. Ryan, G.T. Dee, Macromolecules 34 (2001) 8968.
[19] G. Reiter, G. Castelein, J.U. Sommer, A. Röttele, T. Thurn-Albrecht, Phys. Rev. Lett. 87 (2001) 6101.
[20] A. Röttele, T. Thurn-Albrecht, J.U. Sommer, G. Reiter, Macromolecules 36 (2003) 1257.
[21] P.C. Ashman, C. Booth, D.R. Cooper, C. Price, Polymer 16 (1975) 897.
[22] L. Zhu, S.Z.D. Cheng, B.H. Calhoun, Q. Ge, R.P. Quirk, E.L. Thomas, B.S. Hsiao, F. Yeh, B. Lotz, Polymer 42 (2001) 5829.
[23] A.J. Ryan, J.P.A. Fairclough, I.W. Hamley, S.M. Mai, C. Booth, Macromolecules 30 (1997) 1723.
[24] Y. Mohajer, G.L. Wilkes, I.C. Wang, J.E. McGrath, Polymer 23 (1982) 1523.
[25] I.W. Hamley, J.P.A. Fairclough, F.S. Bates, A.J. Ryan, Polymer 39 (1998) 1429.
[26] R.E. Cohen, A. Bellare, M.A. Drzewinski, Macromolecules 27 (1994) 2321.
[27] P. Rangarajan, R.A. Register, D.H. Adamson, L.J. Fetters, W. Bras, S. Naylor, A.J. Ryan, Macromolecules 28 (1995) 1422.
[28] S. Nojima, K. Kato, S. Yamamoto, T. Ashida, Macromolecules 25 (1992) 2237.
[29] M. Beiner, H. Huth, Nat. Mater. 2 (2003) 595.
[30] E. Hempel, H. Huth, M. Beiner, Thermochim. Acta 403 (2003) 105.
[31] M. Walther, H. Finkelmann, Prog. Polym. Sci. 21 (1996) 951.
[32] O. Ikkala, G. ten Brinke, Science 295 (2002) 2407.
[33] I.A. Ansari, V. Castelletto, T. Mykhaylyk, I.W. Hamley, T. Itoh, C.T. Imrie, Macromolecules 36 (2003) 8898.
[34] I.W. Hamley, V. Castelletto, Z.B. Lu, C.T. Imrie, T. Itoh, M. Al-Hussein, Macromolecules 37 (2004) 4798.
[35] J. Brandup, E.H. Immergut, Polymer Handbook, Wiley, New York, 1989.
[36] S.S. Rogers, L. Mandelkern, J. Phys. Chem. 61 (1957) 985.
[37] S. Hiller, O. Pascui, H. Budde, O. Kabisch, D. Reichert, M. Beiner, New J. Phys. 6 (2004) 1.
[38] E. Hempel et al., in press.
[39] G.W.H. Höhne, Polymer 43 (2002) 4689.
[40] Y.-L. Loo, R.A. Register, A.J. Ryan, Macromolecules 35 (2002) 2365.
[41] L. Mandelkern, in: J. Mark et al. (Eds.), Physical Properties of Polymers, 3rd ed., Cambridge University Press, Berlin, 1997, pp. 209–315.
[42] S. Adamovsky, C. Schick, Thermochim. Acta 415 (2004) 1.
[43] A.B. Herhold, H.E. King, E.B. Sirota, J. Chem. Phys. 116 (2002) 9036.
[44] B.M. Ocko, X.Z. Wu, E.B. Sirota, S.K. Sinha, O. Gang, M. Deutsch, Phys. Rev. E 55 (1997) 3164.
[45] G. Strobl, Eur. Polym. J. E 3 (2000) 165.